UNDERSTANDING AND MODELING THE CO-CURE OF HONEYCOMB CORE SANDWICH STRUCTURES

Timotei Centea[1], Pavel Simacek[2], Mark Anders[1], Navid Niknafs Kermani[2], Daniel Zebrine[1], Suresh Advani[2], and Steven Nutt[1]

[1]M.C. Gill Composites Center, University of Southern California
3651 Watt Way, VHE-406, Los Angeles, CA 90089

[2]Center for Composite Materials, University of Delaware
101 Academy Street, Newark, DE 19716

ABSTRACT

Honeycomb sandwich structures can be manufactured by co-cure, during which prepreg facesheets are concurrently consolidated and bonded to core using film adhesive. This paper describes the major activities and findings of a research project devoted to understanding the physics of co-cure and to developing a physics-based process model. Experimental analysis methods are described, with findings illustrating governing phenomena, complex defect formation mechanisms, and strategies for successful part production. Model development is described from a top-down perspective, addressing requirements, the chosen approach, sub-model development, and integration. Overall, the paper provides practical insights into co-cure and highlights ongoing work to simulate this manufacturing approach based on physics uncovered through experimental investigation.

1. INTRODUCTION

Honeycomb sandwich structures are produced by joining fiber-reinforced polymer facesheets to a lightweight core. Sandwich construction imparts bending strength and stiffness with little added mass by increasing the cross-sectional area moment of inertia. For this reason, sandwich parts are often used in weight-critical applications, including aircraft, spacecraft, high-performance marine vessels (*e.g.*, racing yachts), and wind turbines [1,2,3]. During production, facesheets can be pre-cured on solid tooling and subsequently bonded to core using a film adhesive. Alternately, prepreg laminates can be cured directly over honeycomb during adhesive bonding. Such "co-cure" allows single-step production, eliminates assembly fixtures, alleviates fitment issues arising from dimensional inaccuracy of pre-cured components, and facilitates processing of complex-shaped parts [1].

However, co-cured structures often exhibit higher defect levels than monolithic parts because the physics governing part quality are complex and process development is difficult. Three challenges exist. First, key relationships between material properties, process phenomena, and microstructural quality of the facesheet-adhesive skin remain unclear because of limited research and available experimental data (compared to conventional prepreg consolidation). Second, defect control strategies developed for monolithic parts have proven less effective or counterproductive for co-cure. Third, few reliable process models for co-cure have been proposed. To address these knowledge

SAMPE Conference Proceedings. Charlotte, NC, May 20-23, 2019. Society for the Advancement of Material and Process Engineering – North America.

and capability gaps, and to enable effective, efficient, and robust manufacture of sandwich structures, the co-cure process must be comprehensively understood and modeled.

1.1 Objectives

This paper summarizes and synthesizes major findings from a multi-year research project focused on understanding the science of honeycomb sandwich co-cure and developing a physics-based model for the process. Here, two specific objectives are pursued:

1. Highlight the physics that determine part quality during co-cure, and provide insights on the effects of material, design, and process development choices.
2. Describe the approach chosen to model co-cure, discuss major challenges, and highlight recent results that illustrate the value added by simulations.

First, experimental analysis of co-cure is described, with main findings used to illustrate both the complexity of the process and the conditions required to produce defect-free parts. Then, the approach of modeling co-cure of sandwich structures is discussed. Each section includes a brief review of literature and references to other publications from this project that expand upon key topics. Collectively, the paper is expected to shed light on a common but challenging process for fabricating composite structures and describe efforts to improve quality of co-cured parts using process simulations.

2. EXPERIMENTAL ANALYSIS OF CO-CURE

2.1 Prior Work

Literature has previously addressed major aspects of prepreg processing [4,5] and adhesive bonding [1,6,7]. These scientific and technical insights are relevant and underlie further analysis. The major additional complexity of co-cure is the coupling between facesheet consolidation, bond-line formation, and the behavior of gas entrapped within honeycomb cells. For successful co-cure, the relationships between these processes must be understood and adequately controlled.

Prior studies have investigated links between core pressure evolution, prepreg characteristics, process conditions, and part quality, particularly for out-of-autoclave/vacuum bag-only (OoA/VBO) cure. Tavares et al. [8,9,10,11,12] analyzed through-thickness gas flow within prepreg/adhesive skins during co-cure, and the effect of resulting core pressures on facesheet and bond-line quality and mechanical performance. Kratz et al. [13,14,15,16,17,18] explored the influence of material factors (*e.g.*, fiber bed architecture, core material) on core pressure and part quality, highlighting significant variability during transverse gas flow, and assessed challenges arising during scale-up to large, complex structures. Collectively, these studies confirm that the quality of co-cured parts is strongly influenced by the core pressure, but managing core pressure is challenging during VBO cure. Other literature (*e.g.*, [19,20,21]) has further illustrated complex relationships between materials, process choices, and quality. However, a comprehensive description of process physics and broadly applicable strategies for achieving low defect levels have remained elusive.

2.2 Methods

Experiments were conducted to analyze co-cure physics, identify defect formation mechanisms, and develop strategies for producing low-defect parts. In this project, co-cure was defined as an

autoclave process enabling direct control over temperature (T), autoclave pressure (P_a), and bag pressure (P_b) (Figure 1A). VBO cure is included as a subset with $P_a = 101$ kPa. Two core pressure (P_c) cases were considered based on industry use. "Equilibrated" co-cure assumed that bag and core volumes were directly connected (*e.g.*, through open/vented core or a perforated pre-cured facesheet), such that $P_b = P_c$ throughout processing. Conversely, during "sealed" co-cure, P_c was assumed to evolve as a function of thermal expansion, gas transport out of (or into) the core, and volatile off-gassing.

Material characterization was performed on selected prepreg, adhesive, and core. Two aerospace-grade prepregs (Hexcel HexPly® 8552S and Solvay Cycom® 5320-1, reinforced with ACP193PW 3K and T650-3K plain weave carbon fabrics, respectively) as well as two film adhesives (Henkel Loctite® EA9658AERO, with and without a supporting carrier, and Solvay FM309-1M0.5) were evaluated. Thermal analysis results, including cure kinetics, viscosity, and glass transition behavior are reported in Ref. [22]. Moreover, the moisture absorption of two Nomex-based honeycomb cores was assessed through environmental conditioning and mass uptake measurements, and is also reported in Ref. [22].

In situ analysis was used to clarify the nature and rate of process phenomena and their effect on co-cured part quality. A lab-scale apparatus was developed to: (1) replicate autoclave temperature and pressure conditions, and (2) enable direct real-time observation of bond-line evolution [23,24]. The "mini-autoclave" (Figure 1B) consists of a tool plate (280 × 280 mm) with a machined cavity (76 × 76 × 19 mm) containing one or more glass spacers and a transparent window. The tool surface was used to lay up a half-sandwich assembly consisting of prepreg plies and a layer of film adhesive (both approx. 125 × 125 mm), while the honeycomb core (76 × 76 mm) was placed within the pocket, onto the glass spacer. The skin was enclosed within a vacuum bag (*i.e.*, release film, edge breathing dams, breather and a vacuum membrane), and the tool was covered with a solid lid to form a sealed environment outside the bag. Heaters attached to the tool and lid allowed accurate temperature control (20 - 200°C), while ports located within the bag, core, and autoclave allowed measurement and control of pressure (0.1 – 0.4 MPa). During co-cure, the glass window allowed visual observation of bond-line characteristics and direct correlation to process conditions.

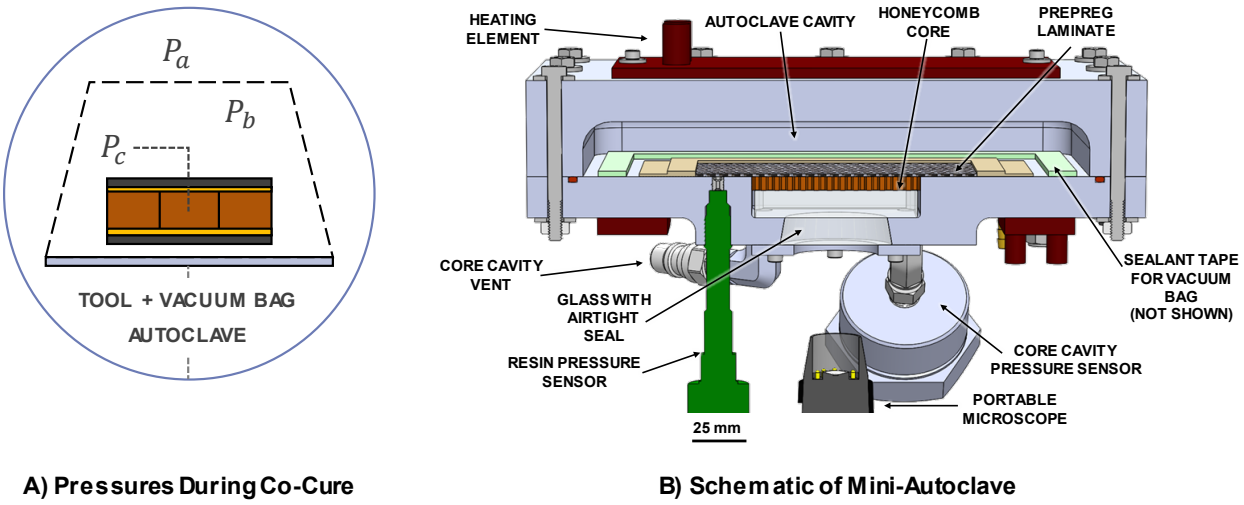

Figure 1: Schematics of (A) pressures during co-cure, (B) the mini-autoclave test fixture, with major components identified using call-out text.

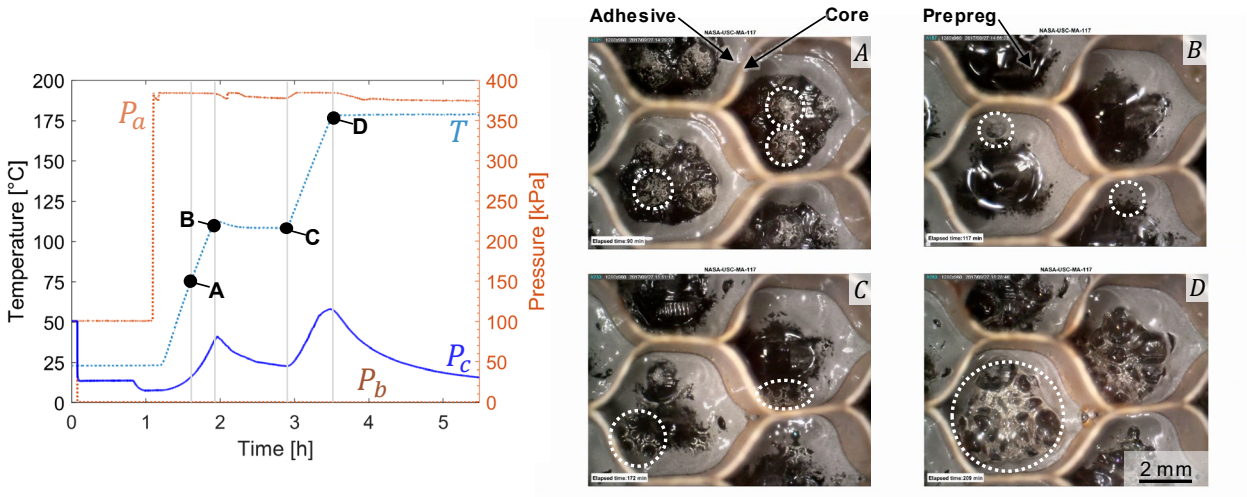

Figure 2: Measured data (T, P_a, P_b, P_c) and *in situ* visual observations of the bond-line for a representative co-cure experiment. The white dotted lines indicate evidence of gas transport or void formation.

The mini-autoclave was used to study diverse co-cure scenarios for both equilibrated and sealed core cases, as described in detail in Refs. [24,25,26,27]. Also, to determine the effective air permeability of facesheets, falling pressure tests were used to measure through-thickness gas flow rates with sealed core cells over a range of temperatures and applied pressures ($P_{app} = P_a - P_b$) [28]. For these tests, the pressure gradient driving resin flow was created by imposing $P_b \cong 0$ kPa and allowing P_c to decrease from 101 kPa towards vacuum. Most recently, co-cures with constant imposed pressure gradients across the bag-side skin were used to assess the effect of gas transport prior to gelation on cured skin permeability [29]. Major findings are summarized in Section 2.3.

2.3 Results: Main Findings

In Situ Analysis. Results from a representative co-cure experiment are shown in Figure 2 [24]. The part consisted of a four-ply prepreg laminate (HexPly® 8552S, PW), a layer of film adhesive (Loctite 9658® AERO UNS), and Nomex core (6.35 mm cells). For this test, the adhesive was reticulated (dewetted over cell walls by heating prior to co-cure) to permit observation of the core-side prepreg ply. The thermal cycle, adapted from manufacturer recommendations for prepreg and adhesive, included a room-temperature vacuum hold (0 – 60 min), a dwell at 110°C (60 min) and a second dwell at 177°C (120 min), with 2°C/min ramps. The autoclave pressure was set to 377 kPa (40 psig) upon heating and the bag pressure was set to 0 kPa (vacuum). The core pressure (sealed) varied with evolving material behavior and process conditions.

Temperature, pressure, and observed microstructural characteristics can be correlated to identify trends. First, P_c decreased upon vacuum application in the bag (due to gas evacuation through the pore network of the uncompacted skin). Then, P_c remained stable during most of the vacuum hold, because the pore network was closed off by compaction, and the effective gas permeability of the skin at ambient temperature was negligible. Nevertheless, during the vacuum hold, air entrapped within the facesheet was observed to slowly migrate into the core through the fabric pinholes, manifesting as bubbles. Upon heating, P_c decreased due to formation of interconnected pores within softening resin regions facilitated by a drop in resin viscosity. Concurrently, lower adhesive viscosity led to fillet formation at skin/core joints and accelerated ingress of air bubbles into the bond-line (Figure 2, Micrograph A). Then, P_c increased during each heat-up ramp because of thermal expansion and moisture release from the core walls but decreased during the dwells due to gas evacuation from core to bag. Void behavior was strongly influenced by these changes. Micrograph B indicates that, at the end of the first heat-up ramp, the fillets had grown larger, but porosity was suppressed by the elevated core pressure. Conversely, micrograph C illustrates that, by the end of the first dwell, lower P_c allowed porosity to grow within both prepreg and adhesive. Finally, micrograph D indicates that, at the end of the heat-up ramp, void growth occurred in the bond-line *despite* a peak in core pressure. This porosity formed mainly in prepreg resin and was attributed to residual solvent within the 8552S resin, elevated temperature, and insufficient resin pressure. These results are representative of a broad set of tests and provide key insights into the physics of co-cure. Entrapped air within facesheets should be evacuated to reduce skin porosity, but it can flow towards the core, rather than the bag, if low P_c creates a favorable gradient. Fillet formation occurs early, once viscosity is sufficiently low to allow wetting flow. The morphology of the adhesive bond-line can be disrupted by porosity, which can nucleate or arise from pre-existing bubbles in the adhesive or core-side prepreg plies (even in cases where adhesive is not reticulated). Voids are strongly influenced by the core pressure, which can evolve non-monotonically with temperature, volatile release, and mass flow out of the core (presuming $P_c > P_b$).

Bond-Line Quality. The effect of P_c on bond-line morphology was studied through trials with the same temperature and autoclave pressure as in the previous example, but with equal bag and core pressures set to levels between 0 kPa and 200 kPa [26]. Three quality regimes were identified (Figure 3). Bond-lines cured with $P_c < 50$ kPa presented little porosity because voids grew and ruptured before gelation (Regime I). However, fillets were small, malformed, and inconsistent. For $P_c = 50$ kPa to 125 kPa (a range that includes ambient pressure, or so-called vented core), fillets exhibited substantial porosity because P_c was too low to prevent void growth (Regime II). However, these entrapped voids led to larger, inflated fillets. Finally, $P_c > 125$ kPa displayed limited

porosity and well-formed fillets owing to suppression of voids by high core pressure (Regime III).

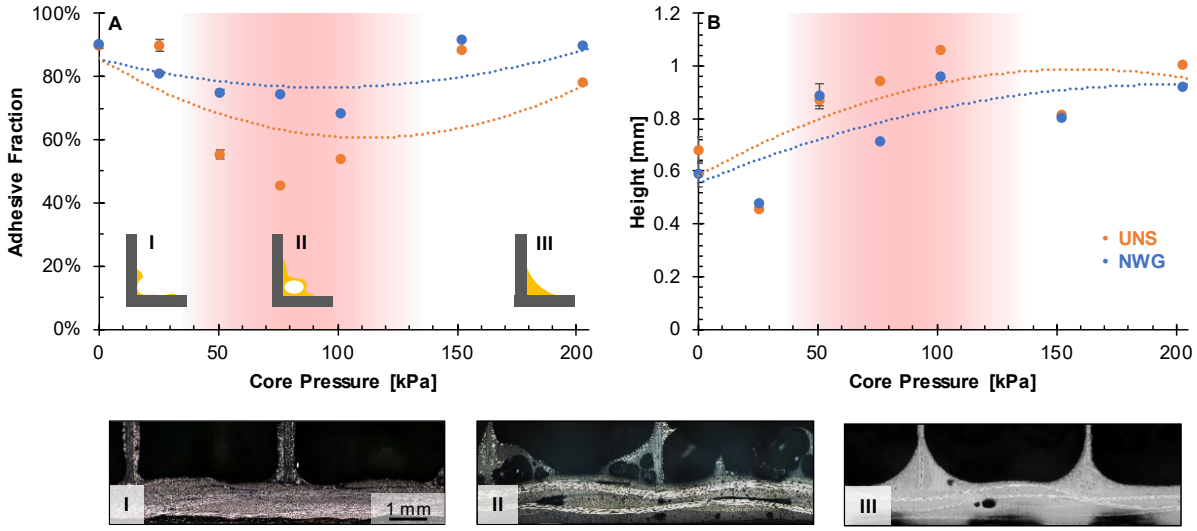

Figure 3: Core pressure effects on (A) adhesive fraction (complement of porosity) and (B) fillet height. The shaded region corresponds to Regime II. The micrographs show fillets associated with Regimes I, II, and III. UNS = unsupported adhesive film, NWG = adhesive film supported by non-woven glass mat

Boundaries defining these regimes are likely material-dependent. However, collectively, this dataset clarifies the physics that underlie the microstructural evolution of the bond-line. Notably, the effect of core pressure on bond-line porosity is non-monotonic: highest porosity is not necessarily observed at lowest P_c, and low porosity does not necessarily correlate with well-formed fillets. Also, observed behavior can exhibit path-dependencies. For example, increasing core pressure *after* void rupture could reduce the size of remaining voids, but would not lead to well-formed fillets because irreversible adhesive redistribution onto cell walls has already occurred. Finally, these results pose questions about bond-line quality control, including (1) whether porosity or fillet shape (or both) are useful metrics of quality and relevant to mechanical performance, and (2) how measurements should be performed, and what threshold values should be used for acceptance.

Facesheet Quality. Prepreg laminates over honeycomb experience complex non-uniform loading, with P_{app} resisted by reaction forces at core walls, in-plane tension within the dimpled facesheet, and the core pressure. Locally within the porous medium, applied loads are shared between the fiber bed effective stress (σ_f) and resin pressure (P_r), both time-dependent. Boundary conditions (BCs) on resin pressure include $P_r = P_b$ at the bag-side limit and $P_r = P_c$ on cell-adjacent surfaces. Thus, if P_r exceeds either P_c or P_b, resin can bleed into core cells or the bag, potentially leading to resin-starved facesheets. Process trials were performed to assess the importance of factors such as the magnitude of P_a, P_b, and P_c, the ply count, and the core cell size on quality metrics such as porosity, dimpling, and fiber volume fraction [25]. Representative data is shown in Figure 4 (values averaged over four polished sections). For the same materials, porosity levels ranged from 1% (for co-cure with *reduced* autoclave pressure, in contrast with the common strategy for monolithic parts) to nearly 4% (for thick facesheets or larger core cells). Dimpling was largely invariant except for a marked increase with larger core cells. Fiber volume fraction changes were less significant than the standard deviation between measurements. Generally, high variability was observed for all spatially-averaged measurements obtained from polished sections because microstructural

characteristics were not uniform, but rather defined by the core geometry (*i.e.*, high compaction and few defects over cell walls, with defects clustered in low-compaction regions over cells). Altogether, these results indicate that material and process factors such as ply count, cell size, and (potentially) process pressures can influence part quality, but that quantitative evaluation is challenging because defects are often localized, and defect levels are spatially non-uniform.

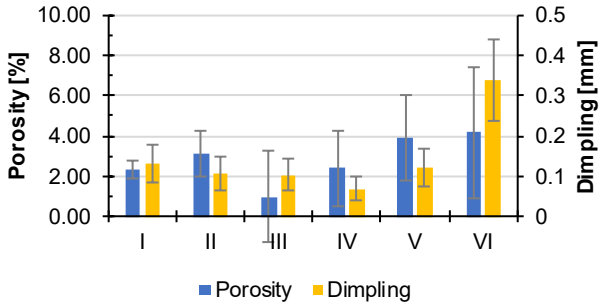

	Plies	Cell Size [mm]	P_a [kPa]	$P_b = P_c$ [kPa]
I	4	3.175	377	0
II	4	3.175	377	**100**
III	4	3.175	**239**	0
IV	4	3.175	**100**	0
V	**8**	3.175	377	0
VI	4	**6.350**	377	0

Figure 4: Facesheet porosity and dimpling data for different ply counts, cell sizes, and process pressures.

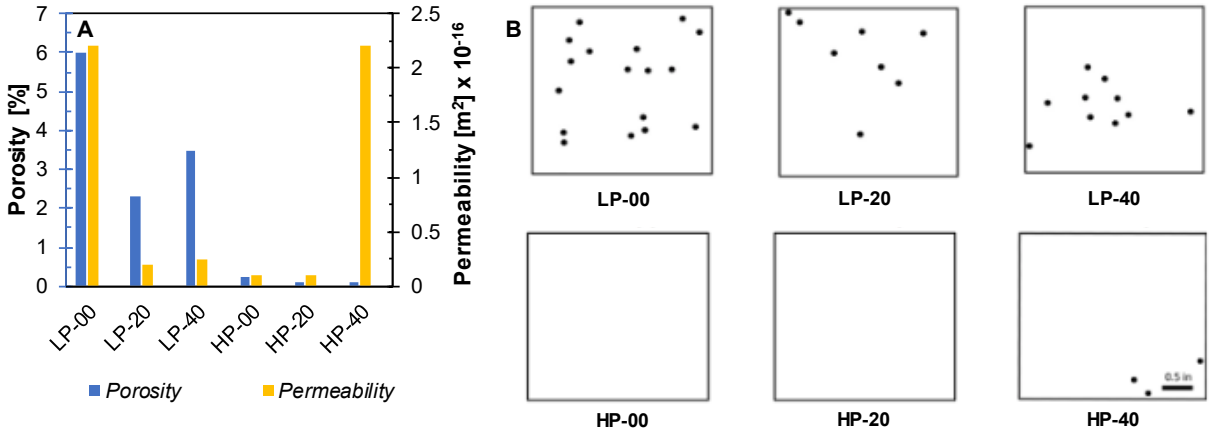

Figure 5: (A) Porosity and transverse permeability of cured skins, and (B) location of surface pinholes.

Skin Permeability. Pressure gradients between gas volumes in the honeycomb and bag can induce formation of gas flow pathways across the facesheet. During co-cure, such flow can affect the core pressure evolution. Moreover, open pore networks can potentially persist after resin gelation, leading to permeable cured skins and increased risk of contaminant ingress during service. Facesheet permeability to through-thickness gas flow during co-cure was measured using falling core pressure tests at multiple temperatures (20 - 90°C) and applied pressures (0.1 – 0.4 MPa) [28]. Pressure decay rates increased substantially at higher temperatures (*e.g.*, by close to two orders of magnitude between 50°C and 90°C) because of lower resin viscosity and decreased with greater applied pressures (though the effect was less significant than that of temperature). *In situ* visual records showed bubble migration through prepreg pinholes, indicating that for this fully-saturated prepreg, gas flow occurred through formation of pathways in resin-rich areas.

Hence, process trials were conducted to assess the effect of through-thickness gas flow on co-cured skin permeability [29]. For simplicity, constant pressure gradients ($\Delta P = P_c - P_b$) were imposed. Two scenarios were considered to isolate the effect of porosity arising from gas flow versus other

factors (low resin pressure, resin starvation). High-porosity (HP) skins were produced using low P_b and P_c, whereas low-porosity (LP) skins were co-cured using super-ambient P_b and P_c, which suppressed porosity (see Figure 3 and upcoming discussion). For each scenario, average ΔP levels of 0, 20, and 40 kPa across the skin were studied. Post-cure, the skin permeability was determined using pressure decay testing, and the microstructure was imaged using polished sections and X-ray tomography. High-porosity skins were permeable, but the magnitude of ΔP during processing did not correlate with permeability in the cured state (Figure 5). Low-porosity parts exhibited no permeability except for $\Delta P = 40$ kPa. Flow visualization using water showed that, for skins with measurable permeability, air traveled through a small number of discrete surface voids. For high-porosity parts, these pinholes connected to large internal pore networks. For low-porosity parts, the surface voids consisted of isolated internal flow channels. The number of surface openings did not correlate closely with gas permeability. Collectively, results show that core-to-bag pressure gradients during co-cure can induce through-thickness gas flow and impart permeability to fabricated skins. Trends also indicate, however, that void content is not a reliable indicator of gas flow rates, because low-porosity skins can exhibit the same permeability as a high-void part. These findings highlight the difficulty of managing process-induced defects during co-cure, and pose challenges for inspection, detection, and criteria for part acceptance.

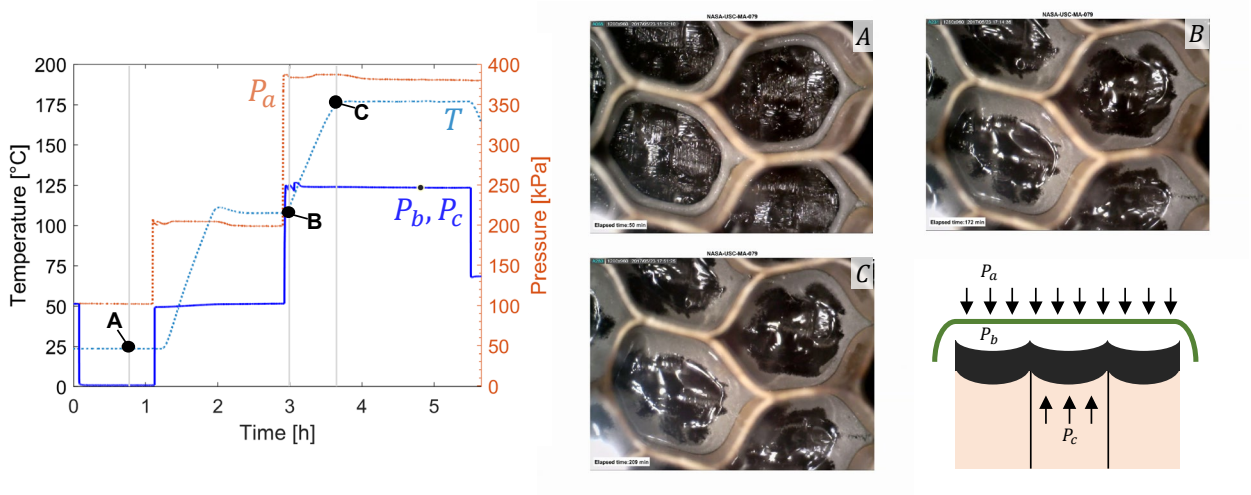

Figure 6: Measured data (T, P_a, P_b, P_c) and *in situ* visual observations of the bond-line for a representative co-cure experiment with in-bag pressurization (IBP).

Strategy for Defect Control. Overall, these findings illustrate key defect formation mechanisms, and clarify the reasons for which conventional defect control strategies (*e.g.*, vacuum-induced air evacuation, higher autoclave pressures) can be ineffective during co-cure. Like conventional prepreg curing, successful processing requires that enough pressure be applied to suppress defects. However, during co-cure, the honeycomb substrate impedes pressure transfer by resisting applied pressure only over core walls and prevents adequate pressure retention by permitting resin bleed into cells. Furthermore, core and bag pressures are often set too low to suppress void growth at exposed surfaces, especially absent pressure transfer from the autoclave.

Given this knowledge, the most direct and effective strategy for co-cure of low-defect parts relies on raising bag and core pressures to levels needed to suppress porosity [24]. Figure 6 shows data from a processing trial during which the autoclave was set to 377 kPa while bag and core pressures were first set to 0 kPa (during the room-temperature hold), then raised to 101 kPa (during the first

dwell), and finally elevated to 239 kPa (during the second dwell). The maximum applied pressure ($P_a - P_b$) for this trial was limited to 138 kPa. Nevertheless, this scenario led to negligible porosity in the facesheet and a uniform, well-formed bond-line because the *minimum* hydrostatic pressure in the system (239 kPa) at gelation was sufficient to prevent defect formation. In-bag pressurization is directly applicable to equilibrated co-cure but can be used for sealed core scenarios if the skin permeability during processing allows equilibration of bag and core pressures (a likely scenario for thin facesheets, based on Ref. [28]). Moreover, by allowing cure of defect-free parts without applied pressures, this method also reduces risk of core crush. Use of in-bag pressurization in production might require modifications to autoclaves and vacuum accessories, but lab-scale work suggest that the approach offers a pathway to reliable fabrication of defect-free parts.

3. MODELING OF CO-CURE

3.1 Prior Work

Models describing aspects of honeycomb sandwich co-cure have been developed but, to date, no comprehensive simulation addressing all key aspects and their interdependencies has been created. Modeling approaches for prepreg consolidation are well-established, and have been previously reviewed (*e.g.*, [4]). However, existing models do not account for specifics of co-cure, including the non-uniform core substrate, the curved (dimpled) shape of the facesheet, and the adhesive bond-line. Rion et al. [21] and Chen et al. [20] derived predictive models for fillet shape and size but did not consider porosity formation. Tavares et al. [9] simulated the progressive saturation and evolving through-thickness permeability of a partially-impregnated facesheet, but did not use predictions to further aims. Kratz et al. [15,16] developed and validated a model for core pressure evolution, accounting for mass transfer into and out of the core (moisture release from Nomex and gas evacuation through the bag-side skin, respectively) and thermal expansion. However, the effect of core pressure on facesheet and bond-line evolution was not simulated.

3.2 Requirements

Process analysis indicates that a physics-based simulation must capture key processes (*i.e.*, core pressure, facesheet, and bond-line evolution) and their coupling. The simulation must also include material models describing the prepreg, adhesive, and core constituents. Finally, for process optimization, modeling must allow users to modify input parameters (*e.g.*, material, temperature, and pressure choices) and evaluate the effect of such changes on a set of useful outputs such as bond-line porosity and degree of prepreg consolidation.

Several challenges arise within this context. Governing equations must respect unique aspects of co-cure, preventing direct use of existing models for monolithic parts. Coupling must be included within the governing equations or numerical solution. Variability from material sourcing, layup protocols, or process physics must be either tolerated by building a model that is sufficiently robust in predicting averages, or addressed by explicitly incorporating stochastic effects (a complex task, not considered here). Finally, the simulation package should be simple to use and easy to improve.

3.3 Approach and Development

Modeling efforts included formulating governing equations, developing requisite sub-models for individual aspects of processing, and creating a framework for implementation and use. In this

paper, modeling is described from a top-down perspective. Further details about model development and planned use are provided in a companion paper [30].

Approach. The project is targeting a stand-alone implementation that simulates relevant process physics for a single core cell (or a set of identical cells) – precluding, for now, challenges related to panel-level modeling (*e.g.*, simulating a 3D domain with spatially-varying temperatures, pressures, and physics). The simpler approach provides two major benefits: fast model evaluation and real-time response, and initial inclusion of variability by simulating cells with different inputs. The organization of the co-cure simulation is shown schematically in Figure 7. Most importantly, sub-models are devoted to distinct process physics, and an explicit implementation allows their modular encapsulation. During numerical solving, sub-models are synchronized at certain time checkpoints by a controller code which transfers needed data between sub-models and advances overall development of process physics to the next time step. Four types of sub-models are used.

Process Description. Model execution requires user-defined material and process data. Currently, users can select among a set of commercially-available pre-characterized prepregs, adhesives, and cores (described in Section 2.2), and define temperature and pressure (P_a and P_b) setpoints.

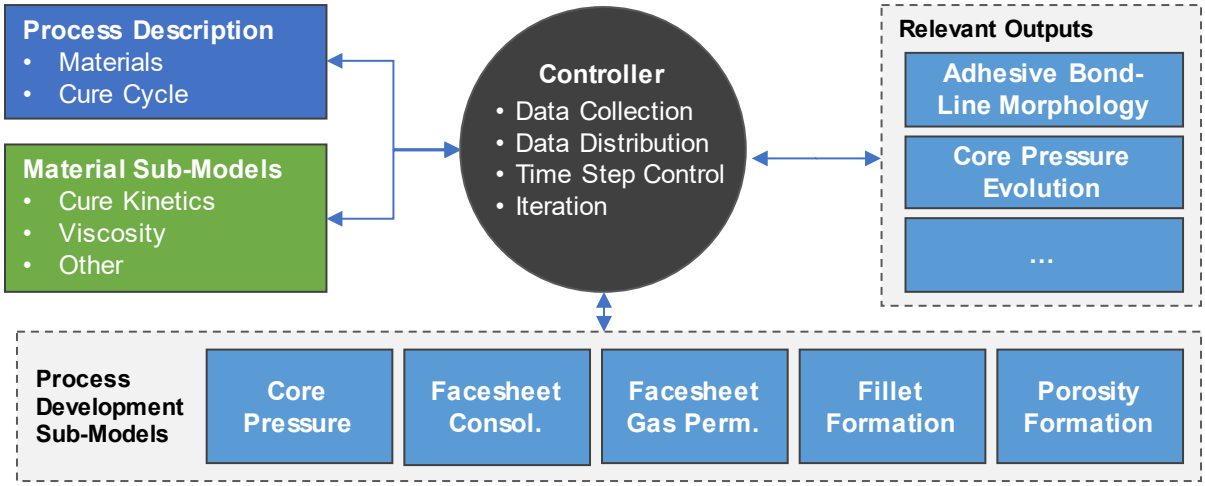

Figure 7: Model organization: process description, materials, process-development, outputs, and controller.

Material Sub-Models. Process description inputs are used to compute required material properties, including degree of cure, viscosity, glass transition temperature, mass loss due to volatile release, and prepreg compliance based on integrated analytical models (including those described in [22]). These datasets are provided as outputs to the user and transferred to other sub-models as needed.

Process Development Sub-Models. Facesheet consolidation, bond-line formation, and evolution of core pressure are simulated based on material and process inputs. Each sub-model is designed to accept input from the controller in the form of relevant material and process data originating from other sub-models (current system state). Then, it executes an internal solution algorithm to model a short term evolution of properties associated with this model based on the inputs provided, and return the useful data (updated component state) to the controller. The generated data is used in other sub-models for subsequent simulations or aggregated for output to user. Full description of

governing equations is beyond the scope of this paper, but a brief overview of major components is presented here, and additional details are available in Refs. [30,31]

Core pressure evolution is determined according to panel set-up (equilibrated or sealed), process cycle, and material properties. For the equilibrated case, $P_c = P_b$, rendering this sub-model trivial. For sealed cores, P_c is calculated using the ideal gas law and a mass balance (Figure 8A, following [16]), accounting for outflow ($\dot{m}_{out}$, air evacuation through the bag-side skin) and inflow ($\dot{m}_{in}$, volatile release from prepreg, adhesive, and core). Gas evacuation is modeled based on Darcy's Law, with the instantaneous effective through-thickness gas permeability of the skin estimated from an empirical (experiment-based) map related permeability to resin viscosity (*i.e.*, temperature) and applied pressure at the required time step (*e.g.*, Figure 8B). Volatile releases from prepreg and adhesive are computed through rate equations developed from thermogravimetric (TGA) experiments, whereas moisture release from Nomex core is estimated using Fickian diffusion equations (following [16]). Case studies have shown that mass transport is most affected by the through-thickness permeability of the bag-side skin. Moreover, while volatile release is material-specific, the extent of mass inflow is not expected to vary across the panel, assuming consistent process conditions. Models accounting for in-plane mass transfer through core walls were investigated, but results supported the use of simplified (1D) simulation of a single cell. If variability is to be considered, a collection of similar cells with varying parameter(s) may be simulated.

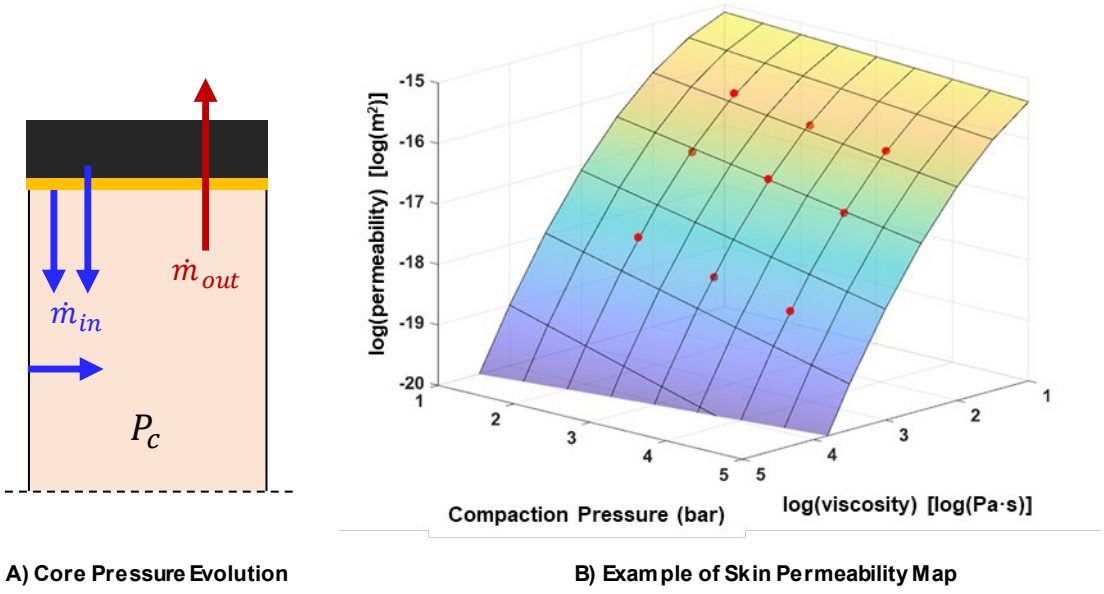

Figure 8: (A) Simplified schematic of core pressure evolution sub-model, and (B) example of instantaneous through-thickness skin permeability map (based on empirical measurements).

Facesheet consolidation over honeycomb core is modeled using a single phase (no independent volatile transport) flow-compaction model in 2D with appropriate BCs. Prepreg is represented as a curved domain supported, at two extremities, by core cells. Boundary conditions include prescribed resin pressures on the bag side (equal to P_b) and core side (P_c), and compaction stresses applied to the fiber bed on the bag side ($P_a - P_b$) and core side (equal to zero). To ensure force equilibrium, the model includes reaction forces from the cell walls and a non-zero in-plane stress within the dimpled prepreg. Four physical processes can occur: (1) fiber bed deformation, (2) resin

flow relative to fibers, (3) void migration relative to fibers and resin, and (4) volatile dissolution and diffusion within the resin. If porosity is limited, the first two mechanisms describe the development of resin flow and compaction properly. The porosity estimates can still be inferred from the flow and pressure data. With substantial porosity, the amount, distribution, and behavior of the gas phase must be explicitly modeled, incurring substantial computation and characterization costs. Currently, efforts are focused on the simpler two-phase model.

Bond-line development is simulated using separate sub-models for fillet and porosity formation. Fillet shape (without porosity) is estimated by computing the force balance affecting the meniscus and can ultimately be estimated through three parameters: the contact angles associated with the core wall and facesheet interfaces, and a non-dimensional number relating surface tension, gravity, density, and cell diameter. The fillet height is the main output of interest. Porosity growth within the bond-line can influence fillet morphology. However, explicitly simulating the effect of voids on fillet shape is challenging. Fillets and voids exhibit similar length scales, preventing common simplifications relying on void growth within an infinite medium. Moreover, bond-line voids show significant stochastic variability in practice. Therefore, bond-line porosity evolution is computed separately from fillet formation, and used to predict whether the ideal fillet shape will experience significant disruption.
Bond-line porosity modeling is based on equations describing the growth (or shrinkage) of a gas bubble within a viscous medium due to diffusion of a volatile species (*e.g.*, moisture or other). The bubble is assigned a surrounding region of influence, limiting available volatiles and growth. The major parameter affecting growth is the pressure surrounding the fillets (*i.e.*, P_c), and the dissolved gas within the adhesive. The bond-line porosity model is described in more detail elsewhere [30].

Output Sub-Models. The simulation must provide data that is (hopefully) verifiable and relevant to practical use of co-cure. For this project, adhesive joint characteristics (*e.g.*, fillet size, porosity) have been identified as primary outputs. However, additional data (*e.g.*, facesheet characteristics) is presented to the user, given that such data exists in the process development sub-models.

Implementation. A simple tool with a graphical user interface (GUI) has been developed to rapidly configure process description, execute material sub-models, and perform the modeling sequence. Input choices (materials, process conditions) are made through drop-down boxes, tabular entries, or data files. Material properties (*e.g.*, degrees of cure, viscosities) are shown for chosen process cycles to allow first-pass validation. At this stage, parameters for material models can be edited in real-time, allowing users to tweak prepreg, adhesive, or core behavior. Finally, outputs (and data from process development models) are displayed as the simulation sequence is advanced either step-by-step or continuously. Data supplied to the user can be exported as graphs or text files. This packaging, while still a rudimentary work-in-progress, provides an indication of the planned capacities and potential use of the co-cure model. Additional details are provided in [30].

4. CONCLUSIONS

This paper summarized activities and synthesized findings from a multi-year research effort to understand the governing science of honeycomb sandwich co-cure and develop a physics-based process model. Experimental work spanned material characterization and process analysis with *in situ* monitoring and observation for diverse co-cure scenarios. These efforts led to valuable insights

into key physical phenomena, clarified defect formation mechanisms, and identified viable strategies for successful processing. Notably:

- Honeycomb sandwich co-cure is governed by several interdependent process phenomena, including core pressure evolution, facesheet consolidation, and bond-line formation. This coupling obscures the effect of material or process changes, introduces path-dependencies, reduces the effectiveness of traditional defect reduction strategies (*e.g.*, raising autoclave pressure), and renders process optimization more challenging.
- Production of sandwich structures with low defect levels involves the same requirements as processing of monolithic prepreg parts: (1) evacuating entrapped air and/or (2) applying enough consolidation pressure to compact the fiber reinforcement and collapse porosity. During co-cure, major challenges include limiting resin pressure loss through bleed into the core, and preventing void growth at free interfaces (*e.g.*, adhesive and core-adjacent prepreg plies). In-bag pressurization addresses both concerns by increasing the minimum pressure within the system to the level needed to prevent defects and allows production of high-quality parts with comparatively reduced applied pressures.

Model development activities focused, concurrently, on developing or adapting physics-based sub-models to describe individual aspects of co-cure (*e.g.*, core pressure evolution, fillet formation and void growth in the bond-line, facesheet consolidation) and creating a framework for coupling and executing these sub-models. Overall, the co-cure simulation, still in development, will allow users to input material and process data, compute material properties, model process phenomena, and estimate likelihood of manufacturing success through relevant outputs (such as fillet shape/size, porosity, and others).

Next steps consist of verification, validation, and improvement of the physics-based simulation by comparison to lab-scale data and scale-up studies (from the authors or external sources). Currently, an alpha-stage version of the simulation software tool capable of simulating equilibrated co-cure is being verified by the academic teams and industry collaborators. Upcoming release of the software will add the capacity to simulate co-cure with sealed core, improve accuracy through revisions to individual sub-models, and enhance ease of input/output.

Collectively, this work responds to challenges and needs related to fabrication of high-performance composites. First, efforts to understand process physics address persistent gaps in knowledge about defect formation in complex structures, and provide guidelines that can help increase part quality, reduce certification and production hurdles, and ensure service performance. Second, development of process models supports a transition towards digital, knowledge-driven manufacturing that can accelerate material selection, part design, process development, and insertion into service.

5. ACKNOWLEDGEMENTS

This work was supported by NASA NRA NNL16AA13C: "A Physics-Based Process Model for Co-Cure Bonding of Honeycomb Core Sandwich Structures." Thomas Cender (University of Delaware) led development of the multi-phase flow model for prepreg gas permeability. Trisha Palit, Emma Morrissey, Vivek Johnson, and Karissa Hendrie (USC) aided with sample preparation and analysis during their undergraduate research assistantships. Roberto Cano and Brian Grimsley (NASA Langley), Shaahin Amini and Milan Mitrovic (United Technologies Aerospace Systems),

and Wenping Zhao and John Gangloff (United Technologies Research Center) provided valuable input on industrial applications of co-cure and related challenges. Material donations from Solvay (Cytec), Henkel, Hexcel, The Gill Corporation, and Airtech are gratefully acknowledged. Financial support was also provided by the Gill Composites Center at USC.

6. REFERENCES

[1] Campbell, F.C. "Chapter 8 – Adhesive Bonding and Integrally Cocured Structure: A Way to Reduce Assembly Costs through Parts Integration". In *Manufacturing Processes for Advanced Composites*. Elsevier, 2004, 241–301.
[2] Herrmann, A.S., Zahlen, P.C., and Zuardy, I. "Sandwich Structures Technology in Commercial Aviation". In O.T. Thomsen, E. Bozhevolnaya and A. Lyckegaard, eds., *Sandwich Structures 7: Advancing with Sandwich Structures and Materials*. Berlin/Heidelberg:, Springer-Verlag, 2005, 13–26.
[3] Thomsen, O.T. "Sandwich Materials for Wind Turbine Blades -- Present and Future". *Journal of Sandwich Structures and Materials 11*, 1 (2009), 7–26.
[4] Hubert, P. and Poursartip, A. "Review of Flow and Compaction Modelling Relevant to Thermoset Matrix Laminate Processing". *Journal of Reinforced Plastics and Composites 17*, 4 (1998), 286–318.
[5] Centea, T., Grunenfelder, L.K., and Nutt, S.R. "A Review of Out-of-Autoclave Prepregs - Material properties, Process phenomena and Manufacturing Considerations". *Composites Part A: Applied Science and Manufacturing 70*, (2015), 132–154.
[6] Banea, M.D. and da Silva, L.F.M. "Adhesively Bonded Joints in Composite Materials: An Overview". *Proceedings of the Institution of Mechanical Engineers, Part L: Journal of Materials: Design and Applications 223*, 1 (2009), 1–18.
[7] Higgins, A. "Adhesive Bonding of Aircraft Structures". *International Journal of Adhesion and Adhesives 20*, 5 (2000), 367–376.
[8] Tavares, S.S., Michaud, V., and Månson, J.A.E. "Through Thickness Air Permeability of Prepregs during Cure". *Composites Part A: Applied Science and Manufacturing 40*, 10 (2009), 1587–1596.
[9] Tavares, S.S., Michaud, V., and Manson, J.A.E. "Assessment of Semi-Impregnated Fabrics in Honeycomb Sandwich Structures". *Composites Part A: Applied Science and Manufacturing 41*, 1 (2010), 8–15.
[10] Tavares, S.S., Caillet-Bois, N., Michaud, V., and Månson, J.-A.E. "Non-Autoclave Processing of Honeycomb Sandwich Structures: Skin Through Thickness Air Permeability During Cure". *Composites Part A: Applied Science and Manufacturing 41*, 5 (2010), 646–652.
[11] Tavares, S.S., Caillet-Bois, N., Michaud, V., and Månson, J.-A.E. "Vacuum-Bag Processing of Sandwich Structures: Role of Honeycomb Pressure Level on Skin–Core Adhesion and Skin Quality". *Composites Science and Technology 70*, 5 (2010), 797–803.
[12] Tavares, S.S., Roulin, Y., Michaud, V., and Månson, J.-A.E. "Hybrid Processing of Thick Skins for Honeycomb Sandwich Structures". *Composites Science and Technology 71*, 2 (2011), 183–189.
[13] Kratz, J. and Hubert, P. "Processing Out-of-Autoclave Honeycomb Structures: Internal Core Pressure Measurements". *Composites Part A: Applied Science and Manufacturing 42*, 8 (2011), 1060–1065.
[14] Kratz, J. and Hubert, P. "Anisotropic Air Permeability in Out-of-Autoclave Prepregs: Effect on Honeycomb Panel Evacuation Prior to Cure". *Composites Part A: Applied Science and*

Manufacturing 49, 0 (2013), 179–191.
[15] Kratz, J. and Hubert, P. "Vacuum-Bag-Only Co-Bonding Prepreg Skins to Aramid Honeycomb Core. Part II. In-Situ Core Pressure Response using Embedded Sensors". *Composites Part A: Applied Science and Manufacturing 72*, (2015), 219–227.
[16] Kratz, J. and Hubert, P. "Vacuum Bag Only Co-Bonding Prepreg Skins to Aramid Honeycomb Core. Part I. Model and Material Properties for Core Pressure during Processing". *Composites Part A: Applied Science and Manufacturing 72*, (2015), 228–238.
[17] Levy, A., Kratz, J., and Hubert, P. "Air Evacuation During Vacuum Bag Only Prepreg Processing of Honeycomb Sandwich Structures: In-Plane Air Extraction Prior to Cure". *Composites Part A: Applied Science and Manufacturing 68*, (2015), 365–376.
[18] Kratz, J., Genest, M., Preau, M., and Hubert, P. "Vacuum-Bag-Only Prepreg Processing of Honeycomb Structures: From Lab-Scale Experiments to an Aircraft Demonstrator". *Proceedings of the SAMPE 2014 Technical Conference*, Society for the Advancement of Material and Process Engineering (2014).
[19] Nagarajan, S., Menta, V.G.K., Chandrashekhara, K., et al. "Out-of-Autoclave Sandwich Structure: Processing Study". *SAMPE Journal 48*, 4 (2012), 24–31.
[20] Chen, C., Li, Y., Gu, Y., Li, M., and Zhang, Z. "Prediction of the Resin Fillet Size in Honeycomb Sandwich Composites with Self-Adhesive Prepreg Skin". *Journal of Reinforced Plastics and Composites 35*, 21 (2016), 1566–1575.
[21] Rion, J., Leterrier, Y., and Månson, J.-A.E. "Prediction of the Adhesive Fillet Size for Skin to Honeycomb Core Bonding in Ultra-Light Sandwich Structures". *Composites Part A: Applied Science and Manufacturing 39*, 9 (2008), 1547–1555.
[22] Centea, T., Zebrine, D., Anders, M., Elkin, C., and Nutt, S. "Manufacturing of Honeycomb Core Sandwich Structures: Film Adhesive Behavior versus Cure Pressure and Temperature". *CAMX 2016 - Composites and Advanced Materials Expo*, (2016).
[23] Anders, M., Zebrine, D., Centea, T., and Nutt, S. "In-Situ Observations and Pressure Measurements for Autoclave Co-Cure of Honeycomb Core Sandwich Structures". *Journal of Manufacturing Science and Engineering*, (2017).
[24] Anders, M., Zebrine, D., Centea, T., and Nutt, S.R. "Process Diagnostics for Co-Cure of Sandwich Structures using In Situ Visualization". *Composites Part A: Applied Science and Manufacturing 116*, (2019), 24–35.
[25] Centea, T., Zebrine, D., Anders, M., and Nutt, S.R. "Facesheet Consolidation During Autoclave Co-Cure of Honeycomb Core Sandwich Structures". *Proceedings of the SAMPE 2017 Technical Conference*, Society for the Advancement of Material and Process Engineering (2017).
[26] Zebrine, D., Anders, M., Centea, T., and Nutt, S.R. "Adhesive Bond-Line Formation During Co-Cure of Honeycomb Sandwich Structures". *Proceedings of the SAMPE 2018 Technical Conference (Student Competition)*, Society for the Advancement of Material and Process Engineering (2018).
[27] Centea, T., Anders, M., Zebrine, D., Nutt, S., and Angeles, L. "The Co-Cure of Honeycomb Sandwich Structures: Process Physics and Manufacturing Strategies". *Proceedings of the 18th European Conference on Composite Materials*, European Society for Composite Materials (2018).
[28] Anders, M., Centea, T., Zebrine, D., et al. "Through-Thickness Gas Permeability of Prepreg Composite Facesheets During Co-Cure of Honeycomb Core Sandwich Structures". *Proceedings of the SAMPE 2018 Technical Conference*, Society for the Advancement of Material and Process

Engineering (2018).
[29] Palit, T., Centea, T., Anders, M., Zebrine, D., and Nutt, S. "Permeability of Cured Composite Skins Produced using Co-Cure over Honeycomb Core". *Proceedings of CAMX 2018 (Student Competition)*, Society for the Advancement of Material and Process Engineering (2018), 1–15.
[30] Niknafs Kermani, N., Simacek, P., and Advani, S.G. "A Simple Tool to Simulate Honeycomb Sandwich Structure Composites During Co-Cure Manufacturing Process". *Proceedings of the SAMPE 2019 Conference*, Society for the Advancement of Material and Process Engineering (2019).
[31] Niknafs Kermani, N., Simacek, P., Erdal, M., and Advani, S.G. "A Numerical Model to Simulate Void Dynamics during Processing of Honeycomb Core Sandwich Structures with Prepreg Face-Sheets". *Proceedings of the 33rd Technical Conference of the American Society for Composites*, American Society for Composites (2018).